

1 **Muscle Precursor Cells enhance the functional Muscle Recovery and show synergistic**  
2 **effects with post-injury treadmill exercise in a muscle injury model in rats.**

3 Paola Contreras-Muñoz<sup>1,2</sup>, Joan Ramón Torrella<sup>3</sup>, Vanessa Venegas<sup>1,2</sup>, Xavier Serres<sup>4</sup>, Laura  
4 Vidal<sup>2</sup>, Ingrid Vila<sup>1,2</sup>, Ilmari Lahtinen<sup>6</sup>, Ginés Viscor<sup>3</sup>, Vicente Martínez-Ibáñez<sup>2</sup>, José Luis  
5 Peiró<sup>2,5</sup>, Tero A.H. Järvinen<sup>6</sup>, Gil Rodas<sup>1,7</sup>, Mario Marotta<sup>1,2,\*</sup>.

6 <sup>1</sup>Leitat Technological Center. Carrer de la Innovació 2, Terrassa, 08225, Barcelona, Spain.

7 <sup>2</sup>Bioengineering, Cell therapy and Surgery in Congenital Malformations Laboratory. Molecular  
8 Biology and Biochemistry Research Centre for Nanomedicine (CIBBIM-Nanomedicine), Vall  
9 d'Hebron Institut de Recerca (VHIR), Universitat Autònoma de Barcelona (UAB), Barcelona,  
10 Spain.

11 <sup>3</sup>Physiology Section, Department of Cell Biology, Physiology and Immunology, Faculty of  
12 Biology, Universitat de Barcelona (UB), Barcelona, Spain.

13 <sup>4</sup>Ultrasound Unit, Department of Radiology, Hospital Universitari Vall d'Hebron, Vall  
14 d'Hebron Institut de Recerca (VHIR), Universitat Autònoma de Barcelona (UAB), Barcelona,  
15 Spain.

16 <sup>5</sup>Translational Research in Fetal Surgery for Congenital Malformations Laboratory. Center for  
17 Fetal, Cellular and Molecular Therapy. Cincinnati Children's Hospital Medical Center  
18 (CCHMC), Cincinnati, Ohio, USA.

19 <sup>6</sup>Faculty of Medicine & Health Technology, Tampere University and Tampere University  
20 Hospital, Tampere, Finland.

21 <sup>7</sup>Medical Services, Futbol Club Barcelona (FCB), Ciutat Esportiva Futbol Club Barcelona, Av.  
22 Onze de Setembre, s/n, 08970 Sant Joan Despí, Barcelona

23 \*To whom correspondence should be addressed: Dr. Mario Marotta, Head of the Regenerative  
24 Medicine laboratory, Health & Biomedicine division, Leitat Technological Center. C/Innovació  
25 nº 2, 08225, Terrassa (Barcelona) Spain. e-mail: [mmarotta@leitat.org](mailto:mmarotta@leitat.org)

26

27 **ABSTRACT:**

28 **Background:** Skeletal muscle injuries represent a major concern in sports medicine. Cell  
29 therapy has emerged as a promising therapeutic strategy for muscle injuries, although the  
30 preclinical data are still inconclusive and its potential clinical use has not yet been established.

31 **Purpose:** To evaluate the effects of Muscle Precursor Cells (MPCs) on muscle healing. MPCs  
32 were administered intramuscularly at 36 h after injury either alone or in combination with 2-  
33 weeks daily post-traumatic exercise training in a rat muscle injury model that mimics skeletal  
34 muscle lesions seen in athletes.

35 **Study Design:** Controlled laboratory study.

36 **Methods:** A total of 27 rats were used in the study. MPCs were isolated from rat (N=3) medial  
37 gastrocnemius muscles and expanded in primary culture. Skeletal muscle injury was induced in  
38 24 rats and the animals were assigned to 3 groups. Injured animals received treatment based on  
39 a single ultrasound-guided MPCs ( $10^5$  cells) injection (Cells group), or the MPCs injection in  
40 combination with 2-weeks daily exercise training (Cells-Exercise group). Animals receiving  
41 intramuscular vehicle injection were used as controls (Vehicle group). Muscle force was  
42 determined 2 weeks after muscle injury and muscles were collected for histology and  
43 immunofluorescence evaluation.

44 **Results:** Red fluorescence-labeled MPCs were successfully transplanted in the site of the injury  
45 by ultrasound-guided injection and localized in the injured area after 2 weeks. Transplanted  
46 MPCs participated in the formation of regenerating muscle fibers as corroborated by the co-  
47 localization of red fluorescence with dMHC-positive myofibers by immunofluorescence  
48 analysis. A strong beneficial effect on muscle force recovery was detected in Cells and Cells-  
49 Exercise groups ( $102.6\% \pm 4.0\%$  and  $101.5\% \pm 8.5\%$  of maximum tetanus force (TetF) of the  
50 injured vs healthy contralateral muscle, respectively) compared to control (vehicle) animals  
51 ( $78.2\% \pm 5.1\%$ ). Both Cells and Cells-Exercise treatments stimulated the growth of newly  
52 formed regenerating muscles fibers, as determined by the increase in myofiber cross-sectional  
53 area ( $612.3 \pm 21.4$  and  $686.0 \pm 11.6 \mu\text{m}^2$ , respectively) compared to vehicle-injected animals

54 (247.5 ± 10.7 μm<sup>2</sup>), that was accompanied by a significant reduction of intramuscular fibrosis in  
55 Cells and Cells-Exercise treated animals (24.2% ± 1.3% and 26.0% ± 1.9% of collagen type I  
56 deposition, respectively) with respect to control animals (40.9% ± 4.1% in Vehicle group).  
57 MPCs-treated muscles induced a robust acceleration of the muscle healing process as  
58 demonstrated by the decreased number of dMHC-positive regenerating (enhanced replacement  
59 of developmental myosin isoform by mature myosin isoforms) myofibers (4.3% ± 2.6% and  
60 4.1% ± 1.5% in the groups Cells and Cells-Exercise, respectively) compared to the Vehicle  
61 group (14.8% ± 13.9%).

62 **Conclusion:** Single intramuscular MPCs administration improves histological outcome and  
63 force recovery of the injured skeletal muscle in a rat injury-model which imitates the sports-  
64 related muscle injuries. Cell therapy showed a synergistic effect when combined with early  
65 active rehabilitation-protocol in rats, and suggests that a combination of treatments can generate  
66 novel therapeutic strategies for the treatment of human skeletal muscle injuries.

67 **Clinical Relevance:** Our study demonstrates the strong beneficial effect of MPC transplantation  
68 and the synergistic effect when the cell therapy is combined with early active rehabilitation-  
69 protocol for muscle recovery in rats, and opens new avenues for the development of effective  
70 therapeutic strategies for muscle healing and clinical trials in athletes undergoing MPC  
71 transplantation and rehabilitation protocols.

72 **Keywords:** Skeletal muscle injury; rat model; MPCs; cell therapy; physical exercise therapy;  
73 muscle healing.

74 **What is known about the subject:** Cell therapy has been postulated as a promising therapeutic  
75 strategy for tissue regeneration and healing. However, few pre-clinical studies have investigated  
76 the effects of intramuscular MPCs transplantation and exercise as potential therapeutic  
77 approaches for muscle healing and there is a lack of consistent pre-clinical data on the MPCs-  
78 therapy alone or in combination with the rehabilitation protocols to support the translation of  
79 MPCs-therapy to the clinical use in humans.

80 **What this study adds to existing knowledge:** We have addressed the individual effects of  
81 intramuscular MPC-injection and its combination with early active rehabilitation in a well-  
82 characterized experimental skeletal muscle injury-model that closely mimics injuries seen in  
83 human athletes. Our study demonstrates the efficacy of the intramuscular MPCs administration  
84 in the healing of injured muscle and reveals that combining it with early active rehabilitation  
85 provides synergistic effects on muscle recovery. Our study can hopefully help to translate the  
86 cell therapy in combination with rehabilitation protocols to the human translational studies.

87

## 88 INTRODUCTION

89

90 Skeletal muscle injuries are the most common sports-related injuries, accounting for up to 55%  
91 of all sports injuries and quite possibly impacting all musculoskeletal traumas <sup>6,17,52</sup>. Although  
92 skeletal muscle demonstrates a remarkable regeneration capacity after injury <sup>38,40</sup>, the healing  
93 process is slow and often results in incomplete functional recovery and an increased risk for  
94 recurrence <sup>25</sup>. Upon injury, the adult muscle tissue activates a complex muscle regeneration  
95 process which is supported by distinct skeletal muscle stem cell populations, namely classical  
96 satellite cells (SCs) and another, more recently identified stem cell population, Muscle-Derived  
97 Stem Cells (MDSCs) <sup>4,10,51</sup>. MDSCs are defined as cells that possess the ability to produce both  
98 new muscle stem cells as well as myoblast and myofiber progeny, without themselves  
99 expressing markers of muscle differentiation. They possess the ability to differentiate into other  
100 cell lineages and have high myogenic capacity to effectively regenerate both skeletal and  
101 cardiac muscle. MDSCs can be stimulated to proliferate and fuse with surrounding myoblasts or  
102 pre-existing myofibers to regenerate damaged muscle tissue and recover muscle functionality  
103 <sup>4,37,58</sup>.

104

105 The transplantation of stem cells into injured tissue in hopes to enhancing the repair process has  
106 long been a central goal of regenerative medicine and tissue engineering. This novel therapeutic  
107 strategy consists of the external supply of progenitor cells to the injured tissue to increase the  
108 number of cells that promote the tissue regeneration. This approach has been previously tested  
109 in the experimental transplantation of myoblasts in animal models of muscle injury and  
110 muscular dystrophy <sup>5,8,16,40,48,55</sup>. Both SCs and MDSCs have been identified as potential  
111 candidates for cell therapy of muscle diseases <sup>15,35</sup>, and their translation for clinical use in  
112 humans is very plausible scenario, since they have the advantage that they can be isolated using  
113 a safe and minimally invasive skeletal muscle biopsy procedure. In addition, the autologous use  
114 of MDSCs has already been evaluated in different clinical trials for the treatment of urinary and  
115 fecal incontinence are ongoing <sup>9,18,51</sup>, although their use in clinical trials for the treatment of

116 skeletal muscle injuries has not yet been initiated. Therefore, to date, only few preclinical  
117 studies have investigated the use of MDSCs for the treatment of acute skeletal muscle injury  
118 <sup>4,27,34,39,42,53</sup>. Based on previously described methodologies<sup>3,19,36,47,59</sup>, we obtained a cell  
119 population of muscle precursor cells (MPCs) with slow adhesion cell characteristics. This stem  
120 cell population, including both SCs and MDSCs, can significantly improve muscle cell-  
121 mediated therapies<sup>43</sup> for the regeneration of injured skeletal muscle by taking advantage of the  
122 healing properties of various types of muscle stem cells present in skeletal muscle tissue.

123

124 Our purpose was to evaluate the potential clinical application of MPCs therapy alone and in  
125 combination with ideal rehabilitation protocol to determine whether the MPC transplantation  
126 improves the healing of the injured skeletal muscle. Thus, we investigated the effects of  
127 ultrasound-guided MPCs transplantation into the site of the injury, and the potential synergistic  
128 effect of combining MPCs transplantation with early, active rehabilitation protocol after injury,  
129 by using a well-characterized experimental skeletal muscle injury-model in rats which  
130 reproduces the injuries seen in human athletes<sup>13,14</sup>. To do this, we designed a preclinical study  
131 to evaluate the individual effects of MPCs transplantation alone or in combination with early  
132 active rehabilitation in our rat muscle injury-model.

## 133 **METHODS**

134

### 135 **Animals, Surgery, and *in vivo* MPCs transplantation**

136 Twenty-four male (8-week-old) Wistar rats (Harlan) were maintained at 22°C with a 12:12 h  
137 light-dark cycle with water and food *ad libitum*. All procedures were performed in accordance  
138 with national (Royal decree 53/2013) and European (2010/63/UE) legislation. All animals  
139 followed a running treadmill training protocol during a 2-week training period, as previously  
140 described<sup>14</sup>. After 2 weeks of pre-injury training, animals were subjected to surgically-induced  
141 skeletal muscle injury in the medial gastrocnemius muscle as described<sup>13</sup>. Briefly, rats were  
142 anaesthetized with a mixture of ketamine (75 mg/kg, intraperitoneally [ip]) and xylazine (10  
143 mg/kg, ip) before the surgical procedure. The muscle injury was generated by using an 18-gauge  
144 biopsy needle (Bard Monopty Disposable Core Biopsy Instrument, Bard Biopsy Systems). A  
145 transverse biopsy procedure was performed at the myotendinous junction level of the right leg  
146 medial gastrocnemius muscle (3 mm from the start of muscle-tendon junction and 2 mm in  
147 depth), resulting in a muscle injury of approximately 20-30% of the total cross-sectional area of  
148 the medial gastrocnemius muscle. Postsurgical analgesia (buprenorphine 0.01 mg/kg) was  
149 subcutaneously administered to all operated animals.

150 Rats were randomly assigned into three groups after skeletal muscle injury (N = 8 per group):

151 1. Vehicle group (Vehicle): A single ultrasound (US)-guided intramuscular injection of 30 µl  
152 MEM (Minimum Essential Medium; Gibco) in the site of the lesion was administered at 36  
153 hours after injury.

154 2. Cell therapy group (Cells): A single US-guided intramuscular injection of cells suspension (1  
155 x 10<sup>5</sup> MPCs resuspended in 30 µl MEM) was administered at 36 hours after the injury at the site  
156 of the muscle lesion.

157 3. Cell therapy and exercise group (Cells-Exercise): Rats were subjected to a combined  
158 treatment of a single US-guided intramuscular injection of cells suspension (1 x 10<sup>5</sup> MPCs  
159 resuspended in 30 µl MEM) administered at 36 hours after injury and in combination with a

160 daily treadmill exercise protocol for 2 weeks<sup>14</sup>. Cell dose was chosen based on previous studies  
161 of muscle stem cells transplantation into muscle injury models in rodents<sup>4,34,39</sup>.

162 All US procedures were performed by using a portable MyLab ONE US device (Esaote SpA)  
163 and a SL3116 22MHz Linear transducer (Esaote SpA). An experienced radiologist in  
164 musculoskeletal ultrasonography carried out the intramuscular US-guided injections in the rat  
165 model (Supplementary video 1).

166 To prevent immune rejection of implanted MPCs, all rats were subjected to daily oral gavage  
167 administration of Tacrolimus (1.0 mg/kg/day, Cinfa) in combination with Mycophenolate  
168 mofetil (20 mg/kg/day, Mylan) for 15 days, starting the immunosuppressive treatment one day  
169 before muscle injury. The combination of Tacrolimus with Mycophenolate mofetil has already  
170 been demonstrated as an optimal method to suppress potential graft rejection in *in vivo* myoblast  
171 transplantation in muscle injury models in rodents<sup>7,49,50</sup>

172

### 173 **MPCs isolation and culture**

174 MPCs were isolated from rat medial gastrocnemius muscles (N=3) according to previously  
175 method described by Allen et al<sup>3</sup> and incorporating the modifications made by Zwetsloot et al.<sup>59</sup>  
176 and Machida et al.<sup>36</sup> Briefly, animals were euthanized by CO<sub>2</sub> inhalation and excised muscles  
177 were pooled, trimmed of excess connective tissue and fat and minced in sterile PBS (Phosphate-  
178 buffered saline; HyClone) containing 5 µg/ml Amphotericine B solution (Sigma-Aldrich).  
179 MPCs were isolated by enzymatic digestion of muscle fragments by incubating with 1.25 mg/ml  
180 of protease type XIV (Sigma-Aldrich) dissolved in DMEM medium containing 25 mM glucose  
181 and 1% antibiotic-antimycotic for 1 h at 37°C. The digested muscle tissue was then centrifuged  
182 at 1,500 xg for 5 min, resuspended in 10 ml of warm PBS and centrifuged at 500 xg for 10 min.  
183 The collected supernatant were filtered through a 100 µm cell strainer (Corning), centrifuged at  
184 1,500 xg for 5 min, and the MPCs pellet was resuspended in the growth medium Ham's F-10  
185 nutrient mixture (Sigma-Aldrich) containing 20% FBS (Fetal bovine serum; Gibco), 1% CEE  
186 (Chicken Embryo Extract; Seralab) and 1% antibiotic-antimycotic (Gibco). MPCs were cultured  
187 using a pre-plating technique<sup>36,47</sup> and the cells were first seeded for 24 h on tissue culture-



188 treated 60 mm plates (Corning). After 24 h, the supernatant was collected and seeded onto a  
189 Matrigel-coated (1 mg/ml; Matrigel Basement Membrane Matrix, BD Bioscience) 60 mm  
190 culture plate. All cell culture experiments were performed in a humidified incubator with 5%  
191 CO<sub>2</sub> at 37°C (NuAire).

192

### 193 **Cell growth analysis**

194 Primary cultured rat MPCs were trypsinized and counted in triplicates by performing the trypan  
195 blue (Sigma-Aldrich) exclusion test of cell viability using a Neubauer counting chamber  
196 (Thermo Fisher Scientific) under optical microscopy (Olympus IX71 microscope).

197

### 198 **Muscle cells differentiation assay**

199 For the differentiation experiments, MPCs were seeded on a Matrigel-coated 60 mm plate to 70-  
200 80% confluency in growth medium. Then, cultured cells were incubated with differentiation  
201 medium (DMEM:MEM in proportion 3:1, containing 2% HS (Horse serum; Gibco) and 1%  
202 antibiotic-antimycotic) for 10 days to induce cell fusion. Culture medium was daily changed  
203 during the differentiation procedure. All microphotographs and videos were taken using an  
204 Olympus IX71 microscope equipped with a DP70 camera (Olympus).

205

### 206 **Cell transfection to express the fluorescent DsRed2 marker gene**

207 To enable tracking of the cells after implantation into the muscle, MPCs were infected with the  
208 retroviral vector pIRES2-DsRed2 (Clontech) containing the internal ribosome entry site (IRES)  
209 of the encephalomyocarditis virus (ECMV) between the Multiple Cloning Site and the  
210 Discosoma sp. red fluorescent protein (DsRed2) coding region. MPCs were incubated with 10  
211 m.o.i (multiplicity of infection) lentiviral particles dissolved in DMEM with 25 mM glucose for  
212 24 h at 37°C. After infection, DsRed2-positive cells were identified by fluorescence microscopy  
213 using a BX-61 microscope (Olympus) equipped with a DP72 camera (Olympus) and CellSens  
214 Digital Imaging software (version 1.9).

215

## 216 **Measurement of Skeletal Muscle Force**

217 Details of evaluation of skeletal muscle contractile function were previously described <sup>13</sup>. In  
218 brief, rats were anesthetized by an intraperitoneal injection of a mixture of ketamine:xylazine  
219 (75:10 mg/kg). Animals were placed in prone position in a platform to immobilize the limb and  
220 Achilles tendon was separated from the calcaneus and, after extracting the soleus muscle from  
221 the triceps surae to analyze the muscle strength of the gastrocnemius muscle, the tendon was  
222 attached to a force transducer (MLT 1030/D, ADInstruments) connected to a PowerLab/16SP  
223 data acquisition hardware (ADInstruments). The sciatic nerve was then exposed through a  
224 lateral incision on the thigh and connected to an electrode and a stimulator (Stimulus Isolator,  
225 FE180; ADInstruments). Muscle force analysis was determined at a constant room temperature  
226 of 25°-27°C in both right (injured) and left (control) gastrocnemius muscles of each animal.  
227 Maximum tetanus force (TetF) was induced by a train of stimuli (100 Hz, 0.1 ms pulse width  
228 and 5 V) and analyzed using the LabChart v7 software (ADInstruments). Finally, the animals  
229 were euthanized by anesthetic overdose and gastrocnemius muscles were excised, weighed,  
230 frozen in supercooled 2-methylbutane (Alfa Aesar) and stored at -80°C until further analysis.

231

## 232 **Histological and Immunofluorescence Analysis**

233 Frozen gastrocnemius muscles were transversely sectioned (10 µm thick) using a Cryotome  
234 (Leica) at below -20°C and mounted on Poly-L-lysine-coated glass slides (VWR). Consecutive  
235 frozen sections were used for histological and immunofluorescence analysis. For histology,  
236 muscle sections were stained with Harris's hematoxylin (Casa Álvarez) and eosin (Panreac) and  
237 mounted with DPX mounting medium and a coverslip (VWR). For immunofluorescence  
238 analysis, frozen muscle sections were fixed in cold (-20°C) acetone (Sigma-Aldrich) and  
239 immunostained with the primary antibodies rabbit anti-collagen-I (Abcam) and mouse anti-  
240 dMHC (developmental myosin heavy chain; Novocastra), and with secondary antibodies Alexa  
241 Fluor 488 anti-mouse or Alexa Fluor 488 anti-rabbit (Invitrogen). Slides were mounted with a  
242 coverslip and Fluoromount-G mounting medium with DAPI (Southern Biotech).

243

244 **Analysis of Muscle Fiber Cross-sectional Area, dMHC, and Collagen-I Expression**

245 For cross-sectional area (CSA) determination, a total of 200 to 300 fibers per muscle in each  
246 group were counted and measured in collagen type I immunofluorescence microphotographs.  
247 All analyzes and measurements were performed in blinded fashion by the same observer in  
248 order to avoid bias in the results. Area of muscle fibers was calculated based on a ratio of  
249 calibrated pixels to actual size ( $\mu\text{m}$ ). dMHC expression levels were analyzed by measuring the  
250 average signal intensity in dMHC immunofluorescence microphotographs, presented as the  
251 percentage of dMHC-positive area respective to the total area of the image. The degree of  
252 fibrosis was evaluated in collagen type I immunofluorescence images by determining the area of  
253 collagen type I respective to the total area in microphotographs. Three images were randomly  
254 selected within the injured area of every gastrocnemius muscle sample by using a BX-61  
255 microscope (Olympus) equipped with a DP72 camera (Olympus) and CellSens Digital Imaging  
256 software (version 1.9). CSA determination, the signal intensity in dMHC and the percentage of  
257 collagen-I area, were measured using the Image J software (version 1.46; National Institutes of  
258 Health).

259

260 **Western blot analysis**

261 For immunoblotting analysis, twenty consecutive frozen transverse sections (10  $\mu\text{m}$  thick) of  
262 every gastrocnemius muscle at the level of the muscle injury were collected using a Cryotome  
263 (Leica) at below  $-20^{\circ}\text{C}$ . Skeletal muscle tissue samples were resuspended in RIPA buffer (20  
264 mM sodium phosphate, pH 7.4, 140 mM NaCl, 1 mM  $\text{MgCl}_2$ , 1% Triton X-100, 5 mM EDTA,  
265 50 mM NaF, 0.1%  $\beta$ -glycerophosphate and complete protease and phosphatase inhibitor  
266 cocktails (Roche Diagnostics) and homogenized using an Omni TH tissue homogenizer (Omni  
267 International). Samples were centrifuged at 10,000xg at  $4^{\circ}\text{C}$  for 15 min and the supernatants  
268 were used for Western blot analysis. Protein was quantified by the BCA protein assay (Pierce)  
269 and equal amounts of protein from supernatants were electrophoresed on 8% SDS gels and  
270 sequentially transferred to nitrocellulose (Biorad) membranes. After blocking with PBS (pH  
271 7.4) containing 5% dry milk for 1 h at room temperature, membranes were incubated with

272 either 1:500 rabbit anti-dMHC (8087, ProSci Inc.), 1:500 rabbit anti-collagen type I (ab34710,  
273 Abcam) and 1:2000 mouse anti- $\alpha$ -Tubulin (T5168, Sigma) antibodies in PBS containing 5%  
274 dry milk at 4°C for 16 h and washed three times for 10 min with PBS and 0.05% Tween-20  
275 (Dako). Then, membranes were incubated with either HRP-conjugated secondary anti-rabbit  
276 IgG (NA934, Amersham) or anti-mouse IgG (NA931, Amersham) antibody in PBS containing  
277 5% dry milk for 1 h at room temperature and washed three times for 10 min with PBS and  
278 0.05% Tween-20. Chemiluminescence was detected using the Clarity™ chemiluminescence kit  
279 (Biorad) and bands were visualized in an Odyssey Fc (LI-COR Biosciences) detector and  
280 quantified using the Image J software (version 1.46; National Institutes of Health).

281

## 282 **Statistical Analysis**

283 Statistical analysis was performed with IBM SPSS Statistics version 20.0 (IBM). The Shapiro-  
284 Wilk test was used to evaluate normality and homoscedasticity of the data. Paired Student's t-  
285 tests were used to determine statistical significance in comparisons of TetF between right  
286 (injured) and left (control) gastrocnemius muscle in every animal. Differences between right  
287 and left gastrocnemius muscle mass of every animal were also evaluated by paired Student's t-  
288 test. One-way analysis of variance (ANOVA) followed by pairwise multiple comparison  
289 procedures (post hoc Holm-Sidak test) was performed to assess the differences in body mass,  
290 muscle mass, collagen-I percentage and TetF (expressed as percentage of injured vs control  
291 muscle) between the 3 groups of animals. A Kruskal-Wallis test was used to evaluate statistical  
292 significance in nonparametric comparisons between the different groups of animals for  
293 myofiber CSA and dMHC expression. In case of significant differences, a Mann Whitney U test  
294 was used to compare the different groups. Data from dMHC and collagen-I expression in  
295 western-blot analysis were normalised to tubulin and compared between groups by Kruskal-  
296 Wallis and Mann Whitney U tests. Differences were considered significant with a P value less  
297 than 0.05.

298

299 **RESULTS**

300

301 **Muscle and Body Mass**

302 No significant difference in body mass was observed between the study groups at the beginning  
303 or at the end of the experiments (Table 1). In addition, no significant difference was detected in  
304 gastrocnemius muscle mass either intra- or inter-groups of treatment.

	Body Mass (g)		Muscle Mass (g)	
	Initial Body Mass	Final Body Mass		Final GM Mass
Vehicle Group	268.3 ± 20.7	327.7 ± 22.9	Control leg Injured leg	2.1 ± 0.2 2.0 ± 0.2
Cells Group	294.3 ± 19.7	347.47 ± 19.0	Control leg Injured leg	2.3 ± 0.2 2.3 ± 0.1
Cells+Exercise Group	283.1 ± 19.7	320.3 ± 22.5	Control leg Injured leg	2.2 ± 0.1 2.2 ± 0.2

**Table 1. Body weight and gastrocnemius muscle mass.** Anesthetized animals were weighed just before to induce gastrocnemius muscle injury and at the end of the treatments. Right (injured) and left (control) gastrocnemius muscle (GM) were excised and weighed from all the animals just before euthanasia at the end of the treatment period. Values are presented as mean ± SD.

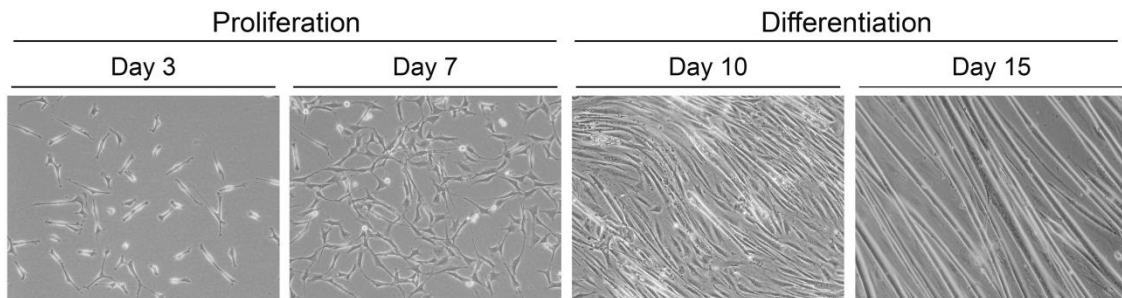
305

306 **Proliferation and differentiation of primary cultured rat MPCs**

307 MPCs were isolated from rat medial gastrocnemius muscles and cultured *in vitro*. Rat MPCs  
308 exhibited spindle-like shape after 3 days in primary culture (Figure 1A, left panel). Four days  
309 later the cell density was significantly increased, more than 4-fold (Figure 1B). In order to  
310 confirm the myogenic properties of the primary cultured MPCs before *in vivo* transplantation,  
311 cells were grown to confluence and induced to differentiate by replacing the proliferation  
312 medium with differentiation medium (Figure 1A, right panel). After 5-7 days in differentiation  
313 medium, MPCs demonstrated the capacity to fuse and form polinucleated myotubes with  
314 spontaneous contractile properties (Figure 1A; Supplementary video 2).

315

A



B

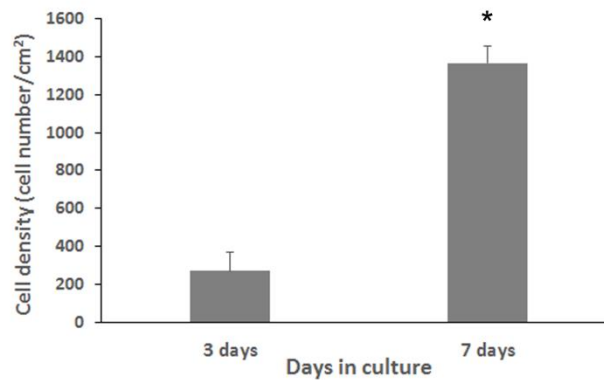


**Figure 1. Myogenic proliferation and differentiation properties of primary cultured rat MPCs.** MPCs were isolated by enzymatic digestion procedures from rat medial gastrocnemius muscle biopsy samples. (A) MPCs expanded in primary culture exhibited spindle-like shape and a strong proliferation and differentiation capacity. Cells were induced to proliferate by incubation in growth medium for 7 days until they reached 70-80% confluence, and then culture medium was changed to differentiation medium to induce the cells to differentiate for 7-8 more days. After inducing differentiation, MPCs demonstrated the capacity to fuse and form multinucleated myotubes with spontaneous contractile properties (see Supplementary video 2). Images show microphotographs at 100x of augmentation obtained under optical microscopy (Olympus IX71 microscope). (B) Cell number of primary cultured rat MPCs was measured by using a Neubauer counting chamber under optical microscopy (Olympus IX71 microscope).

316

317

318 ***In vivo* MPC transplantation into injured site of Medial Gastrocnemius muscle**

319 Next, we induced a focal skeletal muscle injury to medial gastrocnemius muscle and the injured  
320 rats were divided into three groups: Control (Vehicle injection), MPC transplantation group  
321 (Cells), and the group receiving MPCs and treadmill running (Cells-Exercise). Before cell  
322 transplantation, proliferating MPCs were transfected with the retroviral expression vector  
323 pIRES2-DsRed2, which expresses red fluorescent protein, in order to localize cells after  
324 transplantation and to determine whether MPCs would participate in the formation of new  
325 muscle fibers *in vivo*. The efficiency of retroviral infection of MPCs was confirmed by the  
326 presence of red-fluorescence in transfected MPCs cells (Figure 2A). Red-labeled MPCs were  
327 successfully implanted 36 h after muscle injury by intramuscular US-guided injection into the  
328 injured area of medial gastrocnemius muscle (Supplementary video 1). 2 weeks after cell  
329 transplantation, a large number of red-fluorescent (+) muscle cells were detected at the site of  
330 the injury (Figure 2B) in transplanted muscles (Cells and Cells-Exercise groups), but not in  
331 control group. We could not detect transplanted cells outside of the injured area in injured  
332 skeletal muscle.

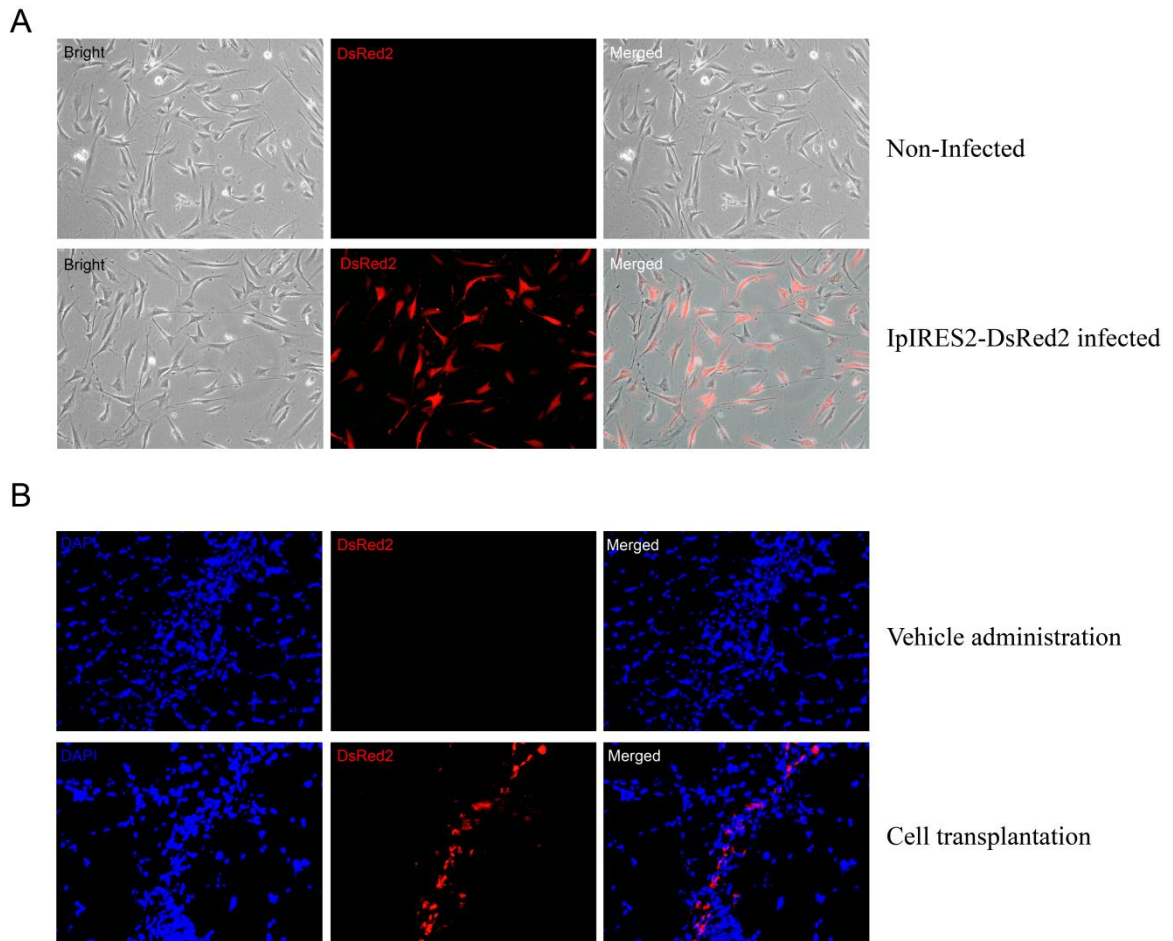


**Figure 2. Localization of red-labelled MPCs before and after intramuscular transplantation. (A)** Before intramuscular transplantation, proliferating MPCs were transfected with the retroviral vector pIRES2-DsRed2 and red-fluorescence in labelled MPCs was confirmed by fluorescence microscopy in cell cultures. **(B)** 2 weeks after cell transplantation by intramuscular US-guided injection into the injured area of medial gastrocnemius muscle, the red-fluorescence(+) labelled muscle cells were successfully detected in cross-sections of medial gastrocnemius transplanted muscles. Images show (x100) microphotographs obtained by using a BX-61 microscope (Olympus) equipped with a DP72 camera (Olympus) and CellSens® Digital Imaging software (version 1.9)

333

334



335 **Effect of Treatments on Gastrocnemius Muscle Force**

336 The effect of the different treatments on muscle force recovery was determined by comparing  
337 the maximum tetanus force (TetF) percentage of injured versus contralateral uninjured muscle  
338 among the different groups of animals.

339

340 The animals in the Vehicle group showed an approximate 22% decrease in TetF of the injured  
341 versus healthy contralateral muscle:  $78.2\% \pm 5,1\%$  ( $P= 0.008$ ) (Figure 3). Both treatments (Cells  
342 and Cells-Exercise groups) produced a strong increase of TetF in the injured muscle with  
343 respect to Vehicle group after 2 weeks of treatment ( $102.6\% \pm 4.0\%$  for MPCs transplantation  
344 group and  $101.5\% \pm 8.5\%$  for combination therapy-group, TetF of the injured vs healthy  
345 contralateral muscle;  $P < 0.001$  vs vehicle group).

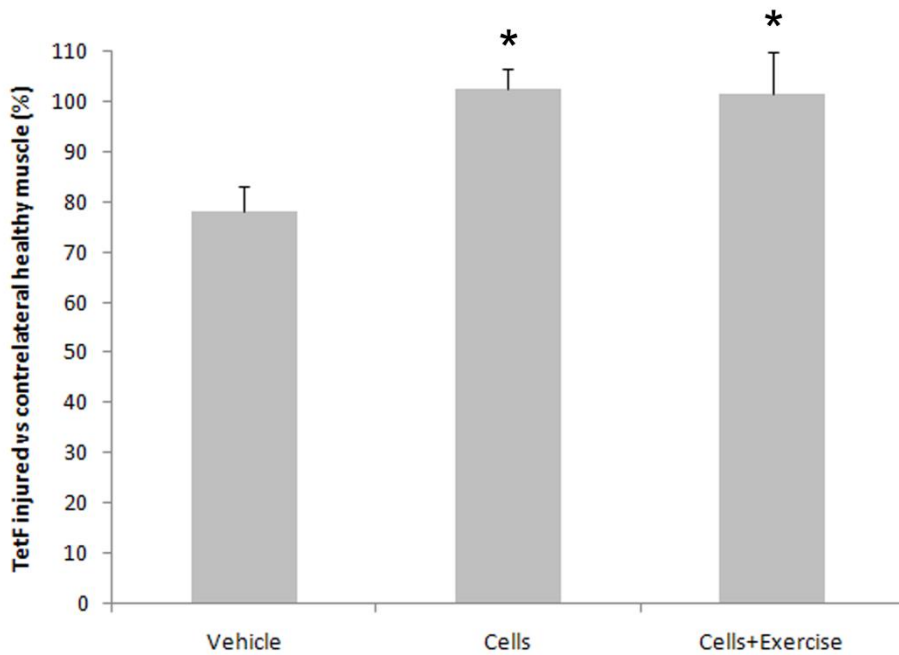


**Figure 3. Measurement of gastrocnemius muscle force after treatments.** Gastrocnemius muscle force was measured at the end of the treatments (14 days post-injury). Data represent maximum tetanus force (TetF) normalized to muscle mass for the injured vs contralateral control muscles. Values are presented as median  $\pm$  SD. \*  $P < 0.01$  vs vehicle-injected group.

346

347

348 **Analysis of muscle regeneration and fibrosis.**

349 Next, we analyzed the cross-sectional area of the myofibers in the injured area after the  
 350 treatment trial. A statistically significant increase in myofiber' CSA was found in rats belonging  
 351 to Cells and Cells-Exercise groups when compared to vehicle-injected animals ( $247.5 \pm 10.7$   
 352  $\mu\text{m}^2$ ;  $P < 0.001$ , Figures 4A and B). Moreover, the Cells-Exercise group showed the largest  
 353 increase in size ( $686.0 \pm 11.6 \mu\text{m}^2$ ) which was significantly higher than in Cells group ( $612.3 \pm$   
 354  $21.4 \mu\text{m}^2$ ;  $P = 0.001$ ) demonstrating a synergistic effect of cell therapy and exercise treatments in  
 355 the treatment of injured skeletal muscle.

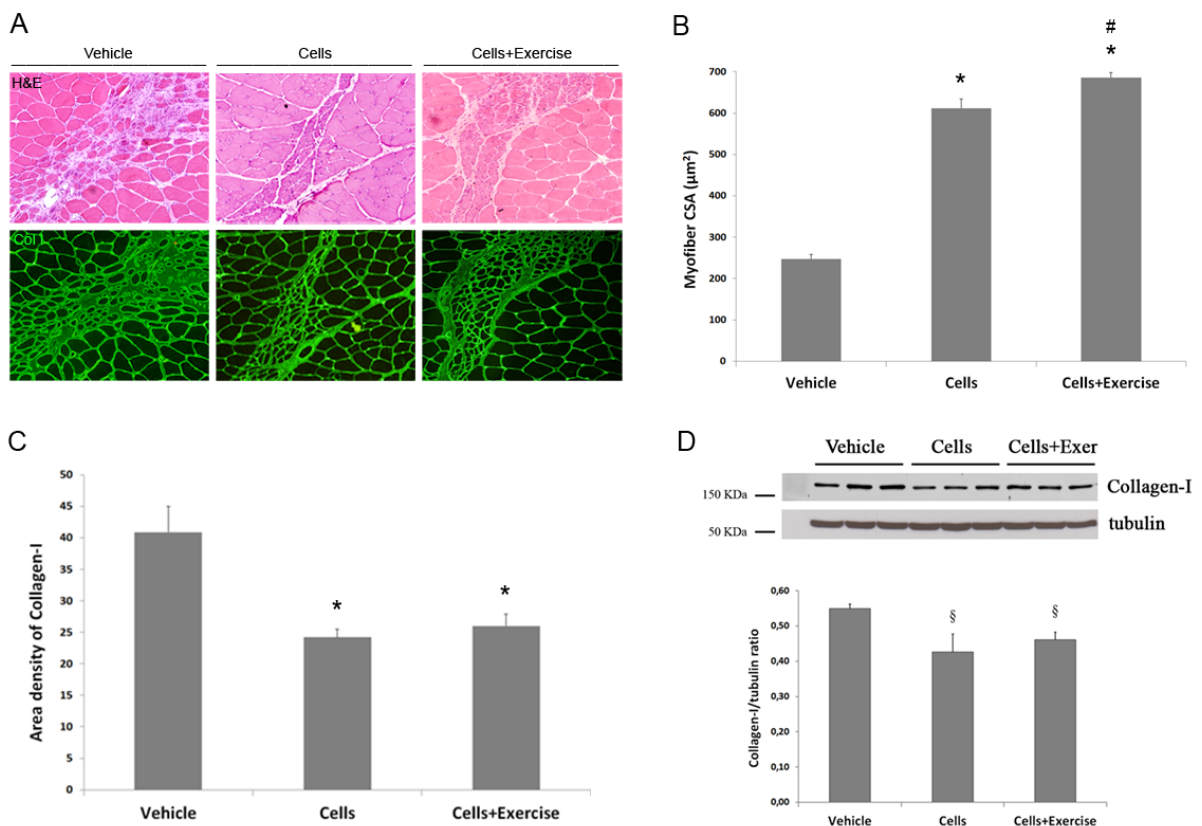


**Figure 4. Analysis of the cross-sectional area of myofibres and degree of fibrosis in rat gastrocnemius muscle.** (A) Representative images (N=8 for each treatment) show Hematoxylin-Eosin stained gastrocnemius muscle cross-sections (upper panel) and immunofluorescence analysis for collagen-I (lower panel) after treatments (14 days post-injury). Images show (x100) microphotographs for all panels. (B) Cross-sectional area (CSA) of newly formed muscles fibres was measured in collagen-I immunofluorescence microphotographs. Three images were randomly selected within the injured area of gastrocnemius muscle cross-sections by using a BX-61 microscope (Olympus) equipped with a DP72 camera (Olympus) and CellSens® Digital Imaging software (version 1.9). The CSA values of 200-300 fibres per muscle were calculated using Image J software version 1.46 (NIH, Bethesda, MD), based on a calibrated pixel-to-actual size ( $\mu\text{m}$ ) ratio. Values are presented as median  $\pm$  SEM. \*  $P < 0.001$  vs vehicle-injected group, #  $P < 0.05$  vs Cells group. (C) The degree of fibrosis was evaluated in Collagen-I immunofluorescence images by determining the area of Collagen-I respecting to the total area in microphotographs. The percentage of collagen-I area was measured by using the Threshold Colour plugin for Image J software version 1.46 (NIH) as an average between 3 and 4 images in every muscle sample. The same threshold set was used for all samples analysed. Values are presented as median  $\pm$  SD. \*  $P < 0.01$  vs vehicle-injected group. (D) Collagen-I expression levels were corroborated by western blot analysis. <sup>§</sup>  $P < 0.05$  vs vehicle-injected group.

356  
357

358

359 The degree of fibrosis was evaluated by the expression of collagen type I in muscle samples  
 360 after 2 weeks of treatment (Figure 4, A and C). The Cells- and Cells+Exercise- groups showed

361 significantly less collagen type I deposition ( $24.2\% \pm 1.3\%$  and  $26.0\% \pm 1.9\%$  of collagen type I  
362 positive area vs total area, respectively) than in vehicle group ( $40.9\% \pm 4.1\%$  of collagen type I  
363 positive area vs. total area,  $P < 0.001$ ). We demonstrated a strong reduction of intramuscular  
364 fibrosis by MPCs transplantation and combining it with exercise therapy (approximately 42%  
365 and 37% decrease in Cells and Cells+Exercise groups, respectively). Collagen type I levels  
366 were also analyzed by western blot analysis (Figure 4D) and we corroborated the decrease in  
367 collagen type I to be 22% ( $P < 0.05$ ) and 16% ( $P < 0.05$ ) in Cells and Cells-Exercise groups  
368 with respect to Vehicle group.

369

370 We then determined the presence of newly formed myofibers during the regeneration process by  
371 immunofluorescence analysis of dMHC expression levels at 2 weeks after treatments (Figure  
372 5A). The participation of the intramuscularly injected MPCs in the formation of newly formed  
373 muscle fibers was corroborated by analyzing the co-localization of the red fluorescence coming  
374 from the injected MPCs and the expression of dMHC (labeled in green fluorescence) detected  
375 by immunofluorescence at the site of the muscle injury (Figure 5A). The co-localization of red  
376 (MPCs) and green (marker of newly forming myofibers) demonstrates that the injected MPCs  
377 are participating in the formation of new muscle fibers to repair the injured muscle segment.  
378 dMHC expression was quantified as the percentage of dMHC-positive area versus total muscle  
379 area in microphotographs (Figure 5B). We found a significant decrease in the number of  
380 dMHC-positive regenerating myofibers in Cells and Cells-Exercise groups ( $4.3\% \pm 2.6\%$  and  
381  $4.1\% \pm 1.5\%$ , respectively) than in Vehicle group ( $14.8\% \pm 13.9\%$ ). The reduction in dMHC  
382 levels was 73% ( $P < 0.001$ ) and 71% ( $P < 0.001$ ) in Cells and Cells-Exercise groups. This  
383 demonstrates the accelerated replacement of the embryonic-developmental myosin isoform by  
384 mature muscle myosin isoforms in regenerating myofibers. No significant differences in dMHC  
385 levels were found between the Cells and Cells-Exercise animal groups. These data were also  
386 corroborated by western blot analysis (Figure 5C) where a reduction of 46% ( $P < 0.05$ ) and 49%  
387 ( $P < 0.05$ ) in dMHC levels was detected in Cells and Cells-Exercise groups with respect to  
388 Vehicle-injected animals.

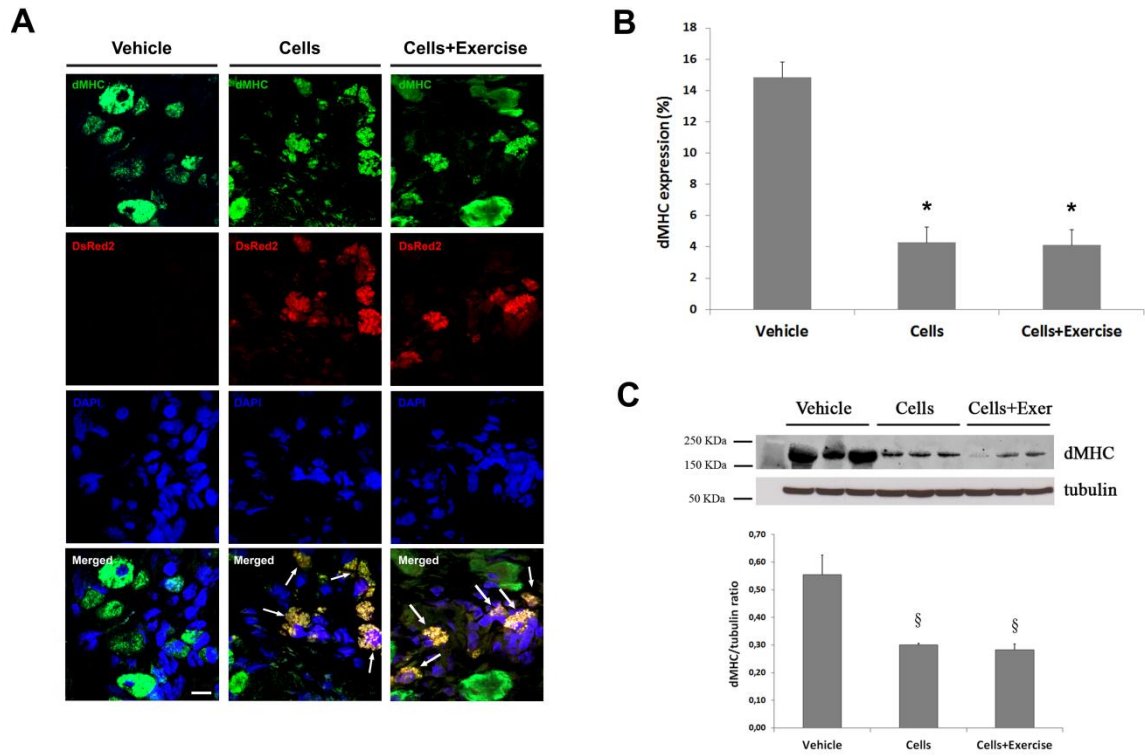


**Figure 5.** Analysis of dMHC expression levels in rat gastrocnemius muscle. (A) Representative images (N=8 for each treatment) show immunofluorescence analysis for dMHC after treatments (14 days post-injury) in gastrocnemius muscle cross-sections. The participation of transplanted MPCs in the formation of new muscle fibres was corroborated by the colocalization (white arrows) of the red fluorescence coming from MPCs with the myotube's marker dMHC analysed by immunofluorescence and labelled in green fluorescence. Images show (x100) microphotographs obtained by using a high resolution LSM 980 with Airyscan confocal microscope (Zeiss) and Zen 3.0 imaging software (version 3.0.79.00004). Scale bar indicates 10  $\mu$ m. (B) dMHC expression levels were analysed by measuring the average green fluorescence signal intensity in dMHC immunofluorescence microphotographs obtained by using a BX-61 microscope (Olympus) equipped with a DP72 camera (Olympus) and CellSens® Digital Imaging software (version 1.9), and the signal intensity was determined by using the Image J software (version 1.46). The dMHC levels are presented as the percentage of dMHC-positive area respecting to the total area of the image. Values are presented as mean  $\pm$  SD obtained from 3 to 4 images of every muscle sample. \* P<0.001 vs vehicle-injected group. (C) dMHC expression levels were corroborated by western blot analysis. § P<0.05 vs vehicle-injected group.

389

390

391 **DISCUSSION**

392

393 We have evaluated the individual effect of MPCs transplantation, and the combination of MPCs  
394 administration with early active rehabilitation protocol, to enhance muscle regeneration in an  
395 experimental rat skeletal muscle injury-model which closely reproduces skeletal muscle strain  
396 injuries seen in human athletes <sup>13</sup>. The advantages of our surgically-induced skeletal muscle  
397 injury animal model in rats include its capacity to reliably induce muscle injuries in rats in a  
398 quick, easy and highly reproducible manner, since it is based in the generation of a transversal  
399 biopsy procedure using identical commercially-available biopsy needles in all the animals for  
400 injury induction. Importantly, our muscle injury model in rats has not only demonstrated to  
401 follow the natural history of muscle regeneration after muscle strain injuries, showing the same  
402 highly orchestrated processes of necrosis, inflammation and regeneration observed in animal  
403 models of spontaneous skeletal muscle strain injury such as the dystrophic mdx-mice, but it has  
404 also demonstrated to imitate the muscle strain injuries observed in the human sports clinics by  
405 the MRI evaluation <sup>13</sup> when MRI images from the rat model were compared to MRI imaging  
406 data from muscle strain injuries in professional athletes <sup>13</sup>.

407

408 MPCs have been postulated as a valuable source of stem cells for therapeutic purposes since  
409 they could be easily obtained from fresh muscle biopsies and isolated in primary cell culture by  
410 sequential enzymatic digestion and pre-plating techniques <sup>11,19</sup>. Although the clinical application  
411 of autologous MPCs transplantation has been already tested in several clinical trials for the  
412 treatment of Duchenne Muscular Dystrophy, sphincter-related urinary or fecal incontinence, and  
413 chronic heart failure diseases <sup>9,18,21,23,51,54</sup>, only few preclinical studies have evaluated the  
414 potential benefits of intramuscular MPCs transplantation for the treatment of skeletal muscle  
415 injuries <sup>4,27,34,39,42,53</sup>. All these clinical applications highlight MPCs as a promising source of  
416 stem cells to develop new therapeutic strategies for the treatment of muscle-related pathologies.

417

418 Skeletal muscle biopsy samples could be easily harvested by means of simple minimally  
419 invasive procedures in an ambulatory clinic environment, providing easy access to muscle stem  
420 cells for their clinical use in musculoskeletal tissue regeneration. Cell culture methodology for  
421 isolating MPCs has been optimized based on the differential adherence of cells by pre-plating  
422 purification techniques<sup>20,24</sup>. This isolation procedure is based on their slow adhesion  
423 characteristics, which leads to the isolation of a purified cell population with a strong myogenic  
424 potential. Before using primary cultured MPCs for intramuscular injection into injured rat  
425 gastrocnemius muscle, we demonstrated their myogenic potential by performing *in vitro*  
426 differentiation analysis. The MPCs demonstrated *in vitro* capacity to fuse and form fully  
427 differentiated myofibers with spontaneous contractile properties (Supplementary video 2) which  
428 corroborates their regenerative potential when used in preclinical studies *in vivo*.

429

430 Our results confirmed the beneficial effect of MPCs-based therapy showing a complete recovery  
431 of the muscle force in all MPCs-treated animals after 14 days of cell transplantation. Since both  
432 groups of animals treated with cells (Cells and Cells+exercise groups) reached the maximum  
433 muscle force at 14 days after treatment, no differences between them were found in TetF  
434 determination. However, the improvement in muscle force was concomitant with the increase in  
435 the size of regenerating myofibers in cell-transplanted animals, since both Cells and Cells-  
436 Exercise groups showed 2.47- and 2.77-fold increase in myofibers' CSA when compared to  
437 vehicle-injected animals. More importantly, we found a synergistic effect of cell therapy when it  
438 was combined with the exercise-based rehabilitation protocol. The combination of both  
439 treatments promoted a significant increase of the size of regenerating myofibers (1.12-fold of  
440 increase in myofibers' CSA in Cells-Exercise group versus Cells group). Our data are in  
441 agreement with previously published data showing the synergistic effect of treadmill running  
442 exercise and intramuscular MPC transplantation to improve skeletal muscle healing in a model  
443 of muscle contusion injury in mice<sup>4</sup>. MPC-based cell therapy not only promoted the growth of  
444 regenerating muscle fibers and muscle force recovery but also accelerated the muscle  
445 regeneration process as demonstrated by the strong decrease in the expression levels of the

446 dMHC, a marker for primitive skeletal muscle fibers. All MPC-treated animals, both Cells and  
447 Cells-Exercise groups, revealed a robust decline (more than 70%) in the number of dMHC-  
448 positive regenerating myofibers when compared to Vehicle group. This finding indicates a  
449 faster replacement of the developmental/embryonic MHC isoform by adult MHC isoforms in  
450 regenerating muscle fibers and demonstrates the acceleration of muscle healing induced by  
451 intramuscular MPCs transplantation. In addition, MSDC-based therapy also induced a strong  
452 reduction of intramuscular fibrosis in both Cells and Cells-Exercise groups of animals, which  
453 showed approximately 40% of decrease of intramuscular collagen type I deposition in the site of  
454 the injury after 2 weeks of treatment. Our results demonstrate the effective anti-fibrotic effect of  
455 intramuscular MPCs administration in the prevention of intramuscular fibrosis and scarring  
456 caused by injury.

457

458 The enhanced muscle regeneration by MPC-therapy could be explained by the substantial  
459 benefits of the external addition of muscle precursor cells at the site of muscle injury during the  
460 first stages of muscle regeneration process. Skeletal muscle activates a self-repair process in  
461 response to injury that is divided in three highly synchronized overlapping phases<sup>10,12,25,26,32</sup>:  
462 inflammation (1-3 days post-injury), regeneration (encompassing up to 3 weeks post-injury and  
463 remodeling phases (3 weeks - 6 months post-injury). During the natural healing process, the  
464 dMHC-positive regenerating myofibers can be detected as soon as at 3 days post-injury, starting  
465 to appear in the periphery of the injured area<sup>13</sup>. This is in line with the activation of muscle  
466 precursor cells that begins within hours after damage. So called *committed* satellite cells  
467 differentiate into myoblast immediately<sup>32,44,57</sup> whereas *stem* satellite cells start to proliferate,  
468 then differentiate into myoblasts and then fuse together to form the newly regenerating muscle  
469 fibers<sup>32,44,57</sup>. It has been reported that the appearance of desmin-expressing myogenic cells can  
470 be detected as soon as after 12 h post-injury in adult rat skeletal muscle injury models<sup>44,57</sup>.  
471 Since the effectiveness of muscle regeneration process is probably directly related to the number  
472 of muscle progenitor cells and myoblasts present in the site of the injury, where they co-exist  
473 with inflammatory cells during the first stages of muscle healing process, the MPC-based

474 therapy by intramuscular transplantation increases the amount of myogenic cells present in the  
475 site of the injury and accelerates the formation of new myofibers and muscle regeneration. This  
476 is of utmost importance as the fundamental problem preventing the injured skeletal muscle  
477 achieving true regeneration is because the regenerating muscle fibers are very poor at extending  
478 to the intertwining scar tissue after they have filled the damaged basal lamina cylinders<sup>1,26,32,56</sup>.  
479 Thus, the scar tissue always develops between the ruptured myofibers in injured skeletal muscle  
480<sup>1,26,32,56</sup>. The addition of exogenous muscle stem cells to the injured area could fill the rupture  
481 area with muscle tissue instead of fibroblast produced scar tissue that would accumulate  
482 between the ruptured muscle fibers without intervention<sup>32</sup>. In addition, taking into account that  
483 the activation of muscle stem cells occurs promptly after muscle damage (during the first days  
484 immediately after the injury), the optimal therapeutic time margin for intramuscular  
485 administration of MPCs could be framed between 24 h and 3 days post-injury, i.e. after the  
486 formation of preliminary fibrin-rich extracellular matrix, which works as a scaffold to retain the  
487 transplanted stem cells between the ruptured muscle fibers. Here, we have demonstrated the  
488 robust beneficial effects of the intramuscular transplantation of MPCs at 36 h post-injury, which  
489 promotes recovery of injured muscle both at functional and structural levels, showing a  
490 complete recovery of muscle force as well as the robust stimulation of regenerating myofibers'  
491 growth in the injured skeletal muscle treated with MPCs.

492

493 Our data demonstrates the *in vivo* synergistic effect of combining intramuscular administration  
494 of MPCs with post-injury exercise-based therapies to promote skeletal muscle healing. Post-  
495 injury exercise has already demonstrated beneficial effects on muscle healing both in humans  
496<sup>22,41,45,46</sup> and animal models of skeletal muscle injury<sup>2,4,14,33</sup>. As previously reported in the  
497 surgically-induced muscle injury rat model, post-injury treadmill running provides substantial  
498 therapeutic effect when given alone, whereas no synergistic effect was detected when exercise-  
499 based treatment was combined with intramuscular Platelet Rich Plasma (PRP) injection<sup>14</sup>.  
500 Unlike the effect of PRP on muscle injuries, which does not add any beneficial effect to early,  
501 active rehabilitation protocols neither in animal models<sup>14</sup> nor in humans<sup>22,45</sup>, MPC-based cell



502 therapy demonstrates a synergistic effect when combined to post-injury exercise to improve  
503 skeletal muscle healing in rats. It may be that the exercise provides the same “regenerative”  
504 stimuli for MPC as it provides for the native cells during the repair of injured skeletal muscle  
505 <sup>31,32</sup>. This may further enhance their biological potential in tissue regeneration.

506

507 A potential limitation of our study, although MPCs have demonstrated an important therapeutic  
508 effect on the treatment of muscle injuries, is that their therapeutic use would require to obtain  
509 them previously as a preventive measure for the application of cell therapy. This is because  
510 obtaining the MPCs requires a muscle biopsy followed by their expansion in the culture for  
511 several days. However, one could push back the injection of MPCs after the inflammatory  
512 period, i.e. after day 3, even though that we used 36 h delay in their administration. This  
513 scenario is supported by previous studies which have demonstrated that skeletal muscle  
514 regeneration does not progress from early myotube formation before the regenerating cells can  
515 use aerobic metabolism as their energy source <sup>28,30</sup>. As the angiogenesis-induced vascular supply  
516 that converts the metabolism of regenerating muscle cells to aerobic takes 5-7 days and the scar  
517 formation does not take place before that <sup>28-30</sup>, the potential therapeutic window of stem cell  
518 therapies could be larger than anticipated. A late transplantation time-point could provide also  
519 benefits such as the improved survival of transplanted stem cells as they would have less hypoxia  
520 to withstand and could have more adherence sites in early, loose granulation tissue that is about  
521 to be produced. Thus, more research is needed to demonstrate the ideal transplantation time-  
522 point of the MPCs in the treatment of skeletal muscle injury, but our positive results encourage  
523 for these future studies. Additionally, regarding the potential transfer of MPC-based cell therapy  
524 to human clinics, based on the results obtained in our rat model and considering the size of  
525 muscle lesions commonly observed in athletes, we estimate that for the transfer of the  
526 therapeutic protocol and escalation to humans, approximately 20-25 million cells would be  
527 needed for intramuscular administration at the site of the injury. Despite the fact that obtaining  
528 tens of millions of cells is very affordable in terms of cell culture and expansion, further  
529 research is needed to establish and optimize the human therapeutic protocol and the precise

530 number of cells to be intramuscularly administered to promote optimal muscle healing and  
531 reduced recovery time in athletes.

532

533 In summary, we have addressed the beneficial effects of intramuscular MPC transplantation and  
534 the potential interaction with early active rehabilitation after injury in a well characterized  
535 experimental skeletal muscle injury-model that closely mimics injuries seen in human athletes.  
536 Our results show that the ultrasound-guided intramuscular MPC transplantation in the site of the  
537 injury at 36 h after skeletal muscle lesion significantly promoted muscle regeneration, decreased  
538 fibrosis formation within the injured muscle and accelerated the functional recovery of the  
539 muscle after injury. Our study also demonstrates the synergistic effect of both MPC-based  
540 therapy and early active rehabilitation-protocol to enhance the repair of the injured skeletal  
541 muscle when these two therapies are combined.

542

## 543 **CONCLUSION**

544 Our results demonstrate beneficial effects of early active rehabilitation-protocol or single  
545 intramuscular MPC-injection on muscle recovery in a rat injury-model which resembles the  
546 sports-related muscle lesions in athletes. We show here that MPC transplantation has a strong  
547 beneficial effect on muscle healing in a surgically-induced muscle injury in rats. In addition, we  
548 have demonstrated *in vivo* the synergistic effect of the combination of both MPC-based therapy  
549 and early active rehabilitation-protocol to stimulate muscle healing after traumatic muscle  
550 injury. The fact that cell therapy and exercise showed beneficial synergistic effects points to  
551 future therapeutic strategies to accelerate muscle healing after injury in athletes subjected to  
552 MPC transplantation and post-injection rehabilitation protocols based on early, active  
553 mobilization.

554

555   **REFERENCES**

556

- 557   1.    Äärimala V, Kääriäinen M, Vaittinen S, et al. Restoration of myofiber continuity after  
558        transection injury in the rat soleus. *Neuromuscul. Disord.* 2004;14(7):421-428.
- 559   2.    Adabbo M, Paolillo FR, Bossini PS, Rodrigues NC, Bagnato VS, Parizotto NA. Effects  
560        of Low-Level Laser Therapy Applied Before Treadmill Training on Recovery of Injured  
561        Skeletal Muscle in Wistar Rats. *Photomed. Laser Surg.* 2016;34(5):187-93.
- 562   3.    Allen RE, Temm-Grove CJ, Sheehan SM, Rice G. Skeletal muscle satellite cell cultures.  
563        *Methods Cell Biol.* 1997;52:155-76.
- 564   4.    Ambrosio F, Ferrari RJ, Distefano G, et al. The Synergistic Effect of Treadmill Running  
565        on Stem-Cell Transplantation to Heal Injured Skeletal Muscle. *Tissue Eng. Part A*  
566        2010;16(3):839-849.
- 567   5.    Bachrach E, Perez AL, Choi Y-H, et al. Muscle engraftment of myogenic progenitor  
568        cells following intraarterial transplantation. *Muscle Nerve* 2006;34(1):44-52.
- 569   6.    Brooks JHM, Fuller CW, Kemp SPT, Reddin DB. Incidence, risk, and prevention of  
570        hamstring muscle injuries in professional rugby union. *Am. J. Sports Med.*  
571        2006;34(8):1297-306.
- 572   7.    Camirand G, Caron NJ, Asselin I TJ. Combined immunosuppression of mycophenolate  
573        mofetil and FK506 for myoblast transplantation in mdx mice. *Transplantation*  
574        2001;72(1):38-44.
- 575   8.    Cao B, Zheng B, Jankowski RJ, et al. Muscle stem cells differentiate into haematopoietic  
576        lineages but retain myogenic potential. *Nat. Cell Biol.* 2003;5(7):640-6.
- 577   9.    Carr LK, Steele D, Steele S, et al. 1-year follow-up of autologous muscle-derived stem  
578        cell injection pilot study to treat stress urinary incontinence. *Int. Urogynecol. J.*  
579        2008;19(6):881-883.
- 580   10.   Chargé SBP, Rudnicki MA. Cellular and molecular regulation of muscle regeneration.  
581        *Physiol. Rev.* 2004;84(1):209-38.
- 582   11.   Chirieleison SM, Feduska JM, Schugar RC, Askew Y, Deasy BM. Human Muscle-

- 583 Derived Cell Populations Isolated by Differential Adhesion Rates: Phenotype and  
584 Contribution to Skeletal Muscle Regeneration in Mdx/SCID Mice. *Tissue Eng. Part A*  
585 2012;18(3-4):232-241.
- 586 12. Ciciliot S, Schiaffino S. Regeneration of mammalian skeletal muscle. Basic mechanisms  
587 and clinical implications. *Curr. Pharm. Des.* 2010;16(8):906-14.
- 588 13. Contreras-Muñoz P, Fernández-Martín A, Torrella R, et al. A New Surgical Model of  
589 Skeletal Muscle Injuries in Rats Reproduces Human Sports Lesions. *Int. J. Sports Med.*  
590 2016;37(3):183-90.
- 591 14. Contreras-Muñoz P, Torrella JR, Serres X, et al. Postinjury Exercise and Platelet-Rich  
592 Plasma Therapies Improve Skeletal Muscle Healing in Rats but Are Not Synergistic  
593 When Combined. *Am. J. Sports Med.* 2017;45(9).
- 594 15. Dellavalle A, Maroli G, Covarello D, et al. Pericytes resident in postnatal skeletal muscle  
595 differentiate into muscle fibres and generate satellite cells. *Nat. Commun.* 2011;2(1):499.
- 596 16. DeRosimo JF, Washabaugh CH, Ontell MP, et al. Enhancement of adult muscle  
597 regeneration by primary myoblast transplantation. *Cell Transplant.* 9(3):369-77.
- 598 17. Dyson R, Buchanan M, Hale T. Incidence of sports injuries in elite competitive and  
599 recreational windsurfers. *Br. J. Sports Med.* 2006;40(4):346-50.
- 600 18. Frudinger A, Marksteiner R, Pfeifer J, Margreiter E, Paede J, Thurner M. Skeletal  
601 muscle-derived cell implantation for the treatment of sphincter-related faecal  
602 incontinence. *Stem Cell Res. Ther.* 2018;9(1):233.
- 603 19. Gharaibeh B, Lu A, Tebbets J, et al. Isolation of a slowly adhering cell fraction  
604 containing stem cells from murine skeletal muscle by the preplate technique. *Nat.*  
605 *Protoc.* 2008;3(9):1501-9.
- 606 20. Guérette B, Asselin I, Skuk D, Entman M, Tremblay JP. Control of inflammatory  
607 damage by anti-LFA-1: increase success of myoblast transplantation. *Cell Transplant.*  
608 6(2):101-7.
- 609 21. Gwizdala A, Rozwadowska N, Kolanowski TJ, et al. Safety, feasibility and effectiveness  
610 of first in-human administration of muscle-derived stem/progenitor cells modified with

- 611           connexin-43 gene for treatment of advanced chronic heart failure. *Eur. J. Heart Fail.*  
612           2017;19(1):148-157.
- 613   22.   Hamilton B, Tol JL, Almusa E, et al. Platelet-rich plasma does not enhance return to play  
614           in hamstring injuries: a randomised controlled trial. *Br. J. Sports Med.* 2015;49(14):943-  
615           950.
- 616   23.   Herreros J, Prósper F, Perez A, et al. Autologous intramyocardial injection of cultured  
617           skeletal muscle-derived stem cells in patients with non-acute myocardial infarction. *Eur.*  
618           *Heart J.* 2003;24(22):2012-20.
- 619   24.   Hodgetts SI, Beilharz MW, Scalzo AA, Grounds MD. Why do cultured transplanted  
620           myoblasts die in vivo? DNA quantification shows enhanced survival of donor male  
621           myoblasts in host mice depleted of CD4+ and CD8+ cells or Nk1.1+ cells. *Cell*  
622           *Transplant.* 9(4):489-502.
- 623   25.   Huard J, Li Y, Fu FH. Muscle injuries and repair: current trends in research. *J. Bone*  
624           *Joint Surg. Am.* 2002;84-A(5):822-32.
- 625   26.   Hurme T, Kalimo H, Lehto M, Järvinen M. Healing of skeletal muscle injury: an  
626           ultrastructural and immunohistochemical study. *Med. Sci. Sports Exerc.* 1991;23(7):801-  
627           10.
- 628   27.   J T, I K, N A, et al. Muscle Derived Stem Cells Stimulate Muscle Myofiber Repair and  
629           Counteract Fat Infiltration in a Diabetic Mouse Model of Critical Limb Ischemia. *J. Stem*  
630           *Cell Res. Ther.* 2016;6(12).
- 631   28.   Järvinen M. Healing of a crush injury in rat striated muscle. 2. a histological study of the  
632           effect of early mobilization and immobilization on the repair processes. *Acta Pathol.*  
633           *Microbiol. Scand. A.* 1975;83(3):269-82.
- 634   29.   Järvinen M. Healing of a crush injury in rat striated muscle. 3. A micro-angiographical  
635           study of the effect of early mobilization and immobilization on capillary ingrowth. *Acta*  
636           *Pathol. Microbiol. Scand. A.* 1976;84(1):85-94.
- 637   30.   Järvinen M. Healing of a crush injury in rat striated muscle. 4. Effect of early  
638           mobilization and immobilization on the tensile properties of gastrocnemius muscle. *Acta*

- 639 *Chir. Scand.* 1976;142(1):47-56.
- 640 31. Järvinen MJ, Lehto MU. The effects of early mobilisation and immobilisation on the  
641 healing process following muscle injuries. *Sports Med.* 1993;15(2):78-89.
- 642 32. Järvinen TAH, Järvinen TLN, Kääriäinen M, Kalimo H, Järvinen M. Muscle injuries:  
643 biology and treatment. *Am. J. Sports Med.* 2005;33(5):745-64.
- 644 33. Kim K, Jun T-W, Kim H, Kim C-J, Song W. Low-intensity treadmill exercise enhances  
645 fast recovery from bupivacaine-induced muscle injury in rats. *Integr. Med. Res.*  
646 2013;2(4):157-165.
- 647 34. Kobayashi M, Ota S, Terada S, et al. The Combined Use of Losartan and Muscle-  
648 Derived Stem Cells Significantly Improves the Functional Recovery of Muscle in a  
649 Young Mouse Model of Contusion Injuries. *Am. J. Sports Med.* 2016;44(12):3252-3261.
- 650 35. Koning M, Harmsen MC, van Luyn MJA, Werker PMN. Current opportunities and  
651 challenges in skeletal muscle tissue engineering. *J. Tissue Eng. Regen. Med.*  
652 2009;3(6):407-415.
- 653 36. Machida S, Spangenburg EE, Booth FW. Primary rat muscle progenitor cells have  
654 decreased proliferation and myotube formation during passages. *Cell Prolif.*  
655 2004;37(4):267-77.
- 656 37. Mackey AL, Kjaer M. The breaking and making of healthy adult human skeletal muscle  
657 in vivo. *Skelet. Muscle* 2017;7(1):24.
- 658 38. Morgan JE, Hoffman EP, Partridge TA. Normal myogenic cells from newborn mice  
659 restore normal histology to degenerating muscles of the mdx mouse. *J. Cell Biol.*  
660 1990;111(6 Pt 1):2437-49.
- 661 39. Ota S, Uehara K, Nozaki M, et al. Intramuscular transplantation of muscle-derived stem  
662 cells accelerates skeletal muscle healing after contusion injury via enhancement of  
663 angiogenesis. *Am. J. Sports Med.* 2011;39(9):1912-22.
- 664 40. Partridge TA, Morgan JE, Coulton GR, Hoffman EP, Kunkel LM. Conversion of mdx  
665 myofibres from dystrophin-negative to -positive by injection of normal myoblasts.  
666 *Nature* 1989;337(6203):176-179.

- 667 41. Pas HIMFL, Reurink G, Tol JL, Weir A, Winters M, Moen MH. Efficacy of  
668 rehabilitation (lengthening) exercises, platelet-rich plasma injections, and other  
669 conservative interventions in acute hamstring injuries: an updated systematic review and  
670 meta-analysis. *Br. J. Sports Med.* 2015;49(18):1197-205.
- 671 42. Proto JD, Tang Y, Lu A, et al. NF- $\kappa$ B inhibition reveals a novel role for HGF during  
672 skeletal muscle repair. *Cell Death Dis.* 2015;6(4):e1730.
- 673 43. Qu-Petersen Z, Deasy B, Jankowski R, et al. Identification of a novel population of  
674 muscle stem cells in mice: potential for muscle regeneration. *J. Cell Biol.*  
675 2002;157(5):851-64.
- 676 44. Rantanen J, Hurme T, Lukka R, Heino J, Kalimo H. Satellite cell proliferation and the  
677 expression of myogenin and desmin in regenerating skeletal muscle: evidence for two  
678 different populations of satellite cells. *Lab. Invest.* 1995;72(3):341-7.
- 679 45. Reurink G, Goudswaard GJ, Moen MH, et al. Rationale, secondary outcome scores and  
680 1-year follow-up of a randomised trial of platelet-rich plasma injections in acute  
681 hamstring muscle injury: the Dutch Hamstring Injection Therapy study. *Br. J. Sports*  
682 *Med.* 2015;49(18):1206-12.
- 683 46. Reurink G, Goudswaard GJ, Tol JL, Verhaar JAN, Weir A, Moen MH. Therapeutic  
684 interventions for acute hamstring injuries: a systematic review. *Br. J. Sports Med.*  
685 2012;46(2):103-9.
- 686 47. Richler C, Yaffe D. The in vitro cultivation and differentiation capacities of myogenic  
687 cell lines. *Dev. Biol.* 1970;23(1):1-22.
- 688 48. Rousseau J, Dumont N, Lebel C, et al. Dystrophin Expression following the  
689 Transplantation of Normal Muscle Precursor Cells Protects mdx Muscle from  
690 Contraction-Induced Damage. *Cell Transplant.* 2010;19(5):589-596.
- 691 49. Skuk D, Goulet M, Roy B TJ. Efficacy of myoblast transplantation in nonhuman  
692 primates following simple intramuscular cell injections: toward defining strategies  
693 applicable to humans. *Exp Neurol.* 2002;175(1):112-126.
- 694 50. Song YX, Muramatsu K, Kurokawa Y TT. Prolonged survival of rat hindlimb allografts

695 following short-course FK506 and mycophenolate mofetil combination therapy.  
696 *Microsurgery*. 2005;25(4):353-359.

697 51. Stangel-Wojcikiewicz K, Jarocha D, Piwowar M, et al. Autologous muscle-derived cells  
698 for the treatment of female stress urinary incontinence: a 2-year follow-up of a Polish  
699 investigation. *Neurol. Urodyn.* 2014;33(3):324-30.

700 52. Stevenson MR, Hamer P, Finch CF, Elliot B, Kresnow M. Sport, age, and sex specific  
701 incidence of sports injuries in Western Australia. *Br. J. Sports Med.* 2000;34(3):188-94.

702 53. Tamaki T, Uchiyama Y, Okada Y, et al. Functional recovery of damaged skeletal muscle  
703 through synchronized vasculogenesis, myogenesis, and neurogenesis by muscle-derived  
704 stem cells. *Circulation* 2005;112(18):2857-66.

705 54. Torrente Y, Belicchi M, Marchesi C, et al. Autologous transplantation of muscle-derived  
706 CD133+ stem cells in Duchenne muscle patients. *Cell Transplant.* 2007;16(6):563-77.

707 55. Torrente Y, Tremblay JP, Pisati F, et al. Intraarterial injection of muscle-derived  
708 CD34(+)Sca-1(+) stem cells restores dystrophin in mdx mice. *J. Cell Biol.*  
709 2001;152(2):335-48.

710 56. Vaittinen S, Hurme T, Rantanen J, Kalimo H. Transected myofibres may remain  
711 permanently divided in two parts. *Neuromuscul. Disord.* 2002;12(6):584-7.

712 57. Vaittinen S1; Lukka R; Sahlgren C; Hurme T; Rantanen J; Lendahl U; Eriksson JE;  
713 Kalimo H. The expression of intermediate filament protein nestin as related to vimentin  
714 and desmin in regenerating skeletal muscle. *J Neuropathol Exp Neurol.* 2001;60(6):588-  
715 97.

716 58. Zammit PS, Partridge TA, Yablonka-Reuveni Z. The skeletal muscle satellite cell: the  
717 stem cell that came in from the cold. *J. Histochem. Cytochem.* 2006;54(11):1177-91.

718 59. Zwetsloot KA, Nedergaard A, Gilpin LT, Childs TE, Booth FW. Differences in  
719 transcriptional patterns of extracellular matrix, inflammatory, and myogenic regulatory  
720 genes in myofibroblasts, fibroblasts, and muscle precursor cells isolated from old male  
721 rat skeletal muscle using a novel cell isolation procedure. *Biogerontology*  
722 2012;13(4):383-398.